Fracture Mechanics of Concrete and Concrete Structures - High Performance, Fiber Reinforced Concrete, Special Loadings and Structural Applications- B. H. Oh, et al. (eds)

Fracture behavior of steel reinforced UHP-SHCC under axial tension

M. Kunieda, M. Hussein, N. Ueda & H. Nakamura
Department of Civil Engineering, Nagoya University, Nagoya, Japan
[*]Post Doctoral Fellow, Department of Civil Engineering, Nagoya University, Nagoya, Japan

ABSTRACT: Ultra High Performance Strain Hardening Cementitious Composites (UHP-SHCC) is a composite material comprising a cement-based matrix and short reinforcing fibers with outstanding mechanical and protective performance. Besides using a thin layer of UHP-SHCC as a protective coating to extend the service life of concrete structures, strengthening of existing reinforced concrete beams with UHP-SHCC layer casted to their soffit may be very successful at restoring or increasing their strength. This type of strengthening noticeably increases both the ultimate load-carrying capacity and the serviceability of reinforced concrete beams. Nevertheless, observed brittle mode of failure of UHP-SHCC-strengthened RC beams and inability of the UHP-SHCC strengthening layer to exhibit a strain hardening behavior is still a concern. Experimental works presented in this paper examine the ability of proposed steel reinforcement to preclude the localized fracture and consequently to improve the post-cracking behavior of UHP-SHCC under axial tension. The dimensions of the practical size test specimens (200 x 50mm) were selected similar to the average value of those used for beams' strengthening applications (thickness = 30 ~ 70 mm).Test results on ten average practical size specimens under axial tension with different reinforcement ratio are reported. Different reinforcement ratios (0.3%, 0.6%, 0.9% and 1.2%) were used to evaluate the reinforcement ratio needed to achieve a target value of ductility.

1 INTRODUCTION

Ultra High Performance Strain Hardening Cementitious Composites (UHP-SHCC) developed by Kunieda et al. (2007) can be simply defined as cement based matrix containing short fibers with higher mechanical and protective performance. Figure 1 shows the general behavior of UHP-SHCC in uniaxial tensile tests compared to that of ordinary SHCC and ordinary Ultra High Performance Fiber Reinforced Concrete (UHPFRC). UHP-SHCC forms a class of cement composites with a tensile stress-strain response that exhibits strain hardening accompanied by multiple cracking. The condition for strain-hardening behavior can be very simply expressed in terms of the post-cracking strength in tension being larger than the cracking strength (Matsumoto & Mihashi 2002). Especially tensile strength of UHP-SHCC is significantly larger (twice or more) than that of ordinary Strain Hardening Cementitious Composites (SHCC). So, it might be one of the effective materials for strengthening of concrete structures. Numerous studies have shown that concrete rehabilitation using ordinary SHCC is very successful at restoring or increasing the load-carrying capacity of concrete members (Horii et al. 1998, Kamal 2008, Kunieda et al. 2006, Maalej & Li 1995, Li 1993, Li 2004, Li 1998, Li et al. 2000, Shin et al. 2007). However, the main downfall of SHCC as a strengthening material is the concentration of cracks developed adjacent to an existing crack in the substrate concrete (Kamal et al. 2008, Kunieda et al. 2004) and the effect of specimen's size on strength and strain capacity. This leads to the fact that: applying the strength values based on the laboratory test using smaller specimens to actual structures may be unconservative.

In this part, reinforcement, which is completely new concept concerning this material, will be explained. Figure 2 shows a schematic image to obtain strain hardening behavior (especially strain capacity) by using strength distribution of both cracking and fiber bridging. Note that, microscopic behaviors related to mechanical properties on cement matrix, fibers and their interface affect the total response.

Figure 2(a) and (b) show the strength distribution of the material with low strain capacity and high strain capacity in the case of strain hardening materials with short fibers, respectively. The difference between cracking strength and fiber bridging strength affects strain capacity. The easiest way to obtain high strain capacity is to increase the volume fraction of fibers, which increases fiber bridging strength. In addition, larger size specimen might increase the width of fiber bridging strength distribu-

tion, which may also decrease strain capacity, and this might be one of the reasons of size effect.

Figure 2 (c) introduces the role of reinforcement in this study. As describe in above, to increase the fiber bridging strength can increase strain capacity, and the reinforcement can help to obtain the high strain capacity based on the concept supporting the fiber bridging.

Based on Figure 3, example of contribution of a reinforcement having the diameter of 6mm will be introduced. Here the bond between the cement material and rebar is assumed to be perfect. Nominal stress increase of cracking strength and fiber bridging strength including rebar contribution are about 0.07MPa (load at 100micro strain/ nominal cross sectional area) and about 1MPa (yielding load/ nominal cross sectional area), respectively. Increment of fiber bridging strength due to additional reinforcement was higher than that of cracking strength, and this may cause multiple fine cracks.

Of course, large amount of reinforcement can also give high strain capacity. However, the target of this study is to ensure the material properties in laboratory tests by using only small amount of reinforcement.

With the above-presented concerns, a comprehensive experimental study is performed to (1) provide experimental data on the structural performance of UHP-SHCC tension members with practical size, (2) measure the ultimate stress and strain of small (dumbbell-shaped specimens) and practical size members to see if they are similar for members of different sizes, and (3) examine the ability of the proposed steel reinforcement to recover the mechanical properties of large size specimens. For this purpose ten practical size UHP-SHCC specimens (tested cross-section: 50x200mm) with different reinforcement ratios, and ten dumbbell-shaped specimens (tested cross-section:13x30 mm) were tested. This study investigates cracking development, strain distribution along the specimen's axis and the effect of varying the steel amount on the specimen's post-cracking behavior.

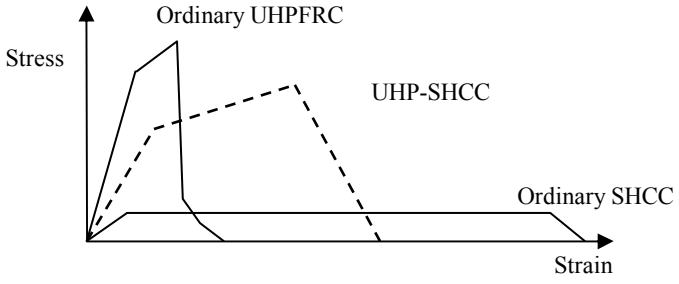

Figure 1. Schematic image of UHP-SHCC material tensile behavior compared to that of other materials (Kamal et al. 2008).

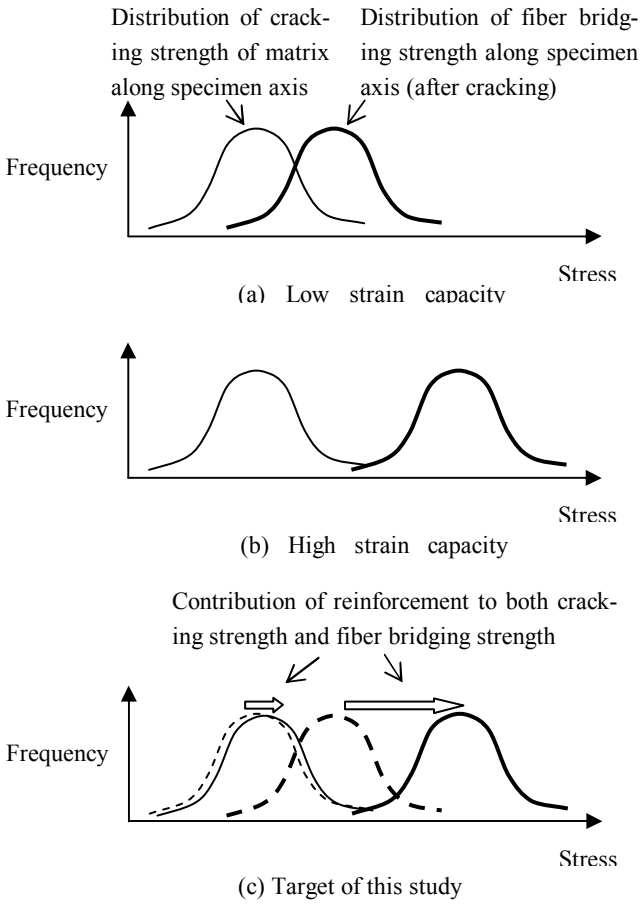

Figure 2. Schematic images of mechanism to obtain strain capacity.

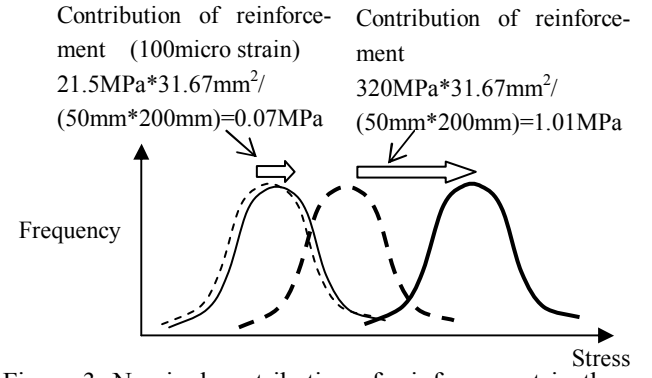

Figure 3. Nominal contribution of reinforcement in the case of 1D6.

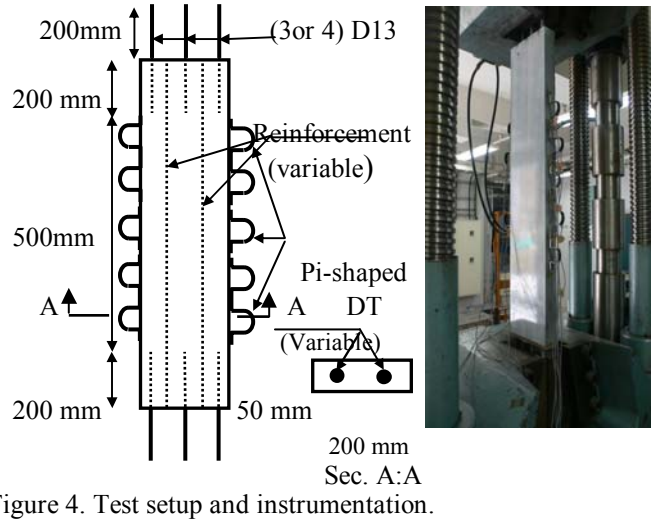

Figure 4. Test setup and instrumentation.

Table 1. Description of tested specimens.

Specimen	Dimensions (mm)	Reinforcement	ρ_s^* (%)	Number of specimens
S-0	50x200x900	-----	0	2
S-1	50x200x900	1D6	0.3	2
S-2	50x200x900	2D6	0.6	2
S-3	50x200x900	3D6	0.9	2
S-4	50x200x900	4D6	1.2	2

* Reinforcement ratio

2 EXPERIMENTAL PROGRAM

2.1 *Test Specimens*

As mentioned before, the present study was carried out to provide experimental data on the structural performance of UHP-SHCC tension members of a practical size. The dimensions of the practical size test specimens (200 x 50mm) were selected similar to the average value of those used for beams' strengthening applications (thickness = 30 ~ 70 mm). Thus, the obtained results may help to provide guidance for further research and development in the field of enhancement of UHP-SHCC-strengthened beams' ductility.

To evaluate the size effect on the crack distributions and the strain capacity, ten dumbbell-shaped specimens (tested cross-section:13 x 30 mm) and two practical-size specimens (tested cross-section 50 x 200 mm) were tested. Also, ten specimens with different reinforcement ratios were tested to examine the ability of the proposed steel reinforcement to preclude localized fracture and to obtain a considerable strain-hardening response. The UHP-SHCC specimen is a 900 mm long prism with a rectangular cross section of 200 x 50 mm. Specimens' depth was selected to provide data on similar thickness of practical repair applications. Rebars of 6 mm diameter (D6) were used as steel reinforcement. To facilitate the application of tensile force, rebars of 13 mm diameter (D13) were placed at the specimens' ends as shown in Figure 4. The embedded lengths and number of D13 rebars required for each specimen were carefully designed to avoid any possible anchorage failure. Four D13 rebars were used for highly reinforced specimen S-4 whereas three D13 rebars were used for all other specimens. Table 1 lists the dimensions, reinforcement ratio, and number of tested specimens.

2.2 *Material properties*

Table 2 lists the mix proportions of UHP-SHCC. The water to binder ratio (W/B) was 0.20. Low heat Portland cement (density: 3.14 g/cm^3) was used, and 15% of the design cement content was substituted with a silica fume (density: 2.2 g/cm^3). Quartz sand (less than 0.2 mm in diameter, density: 2.68 g/cm^3) was used as the fine aggregate. High strength polyethylene (PE) fiber was chosen for UHP-SHCC and the fiber volume in the mix was 1.5%. The diameter and length of the PE fibers were 0.012mm and 6mm, respectively. Superplasticizer was used to enhance the workability of the matrix. After demoulding, all the specimens were covered with wet towels in a special curing room for four weeks. The tensile behavior of the used UHP-SHCC was characterized by testing of ten dumbbell-shaped specimens (tested cross-section: 13 x 30 mm) in uniaxial tensile test, whereas, compression test were performed on six cylindrical specimens having the size of 50x100mm to obtain the UHP-SHCC compression strength. The averaged tensile strength, compressive strength and tensile strain of the UHP-SHCC at the age of 28 days were determined to be 6.5 MPa, 95 MPa and 1.5%, respectively. The averaged yield strength, tensile strength and Young's modulus for the used D6 rebars were 320 MPa, 529 MPa and 215 GPa respectively.

2.3 *Test setup and procedure*

All the large size specimens were tested by applying a tension force according to the test setup shown in Figure 4. The specimens were tested in a tensile testing machine with a capacity of 2,000 kN in a load-controlled way. Tensile force was applied by gripping the steel bars at the specimen's ends. The load was increased gradually until failure occurred. During the test, strains were recorded by ten Pi-shaped displacement transducers with a gauge length and accuracy of 100 mm and 0.005 mm, respectively, which were attached to each surface of the specimen, as shown in Figure 4.

Table 2. Mix proportions of UHP-SHCC.

Material	Water/ binder	Unit content (kg/m3)							
		Water	Cement	Silica fume	Expansion agent	Sand	Super plasticizer	Air reducer	Fiber content (6mm)
UHP-SHCC	0.20	292	1243	223	20	149	14.9	2.98	14.6

Table 3. Experimental results.

Specimen	Load		Cracks					Strain	
	P_{cr}	P_u	$S_{r\text{-}av}$(mm)	$S_{r\text{-}max}$(mm)	N	$\varepsilon_{u\text{-}av}$(%)	$\varepsilon_{u\text{-}max}$(%)	$\varepsilon_{u\text{-}av}/\varepsilon_{cr\text{-}av}$	$\varepsilon_{u\text{-}av}/\varepsilon_{u\text{-}av\text{-}D}$
S-0-1	42	50	12.0	176	43	0.24	0.717	14	0.16
S-0-2	39	47	14.0	185	45	0.23	0.851	13	0.15
S-1-1	42	64	4.6	40	119	1.58	2.377	102	1.05
S-1-2	41	65	4.5	42	118	1.60	2.301	101	1.06
S-2-1	40	74	4.0	10	128	1.49	2.276	103	0.99
S-2-2	40	73	4.0	10	130	1.50	2.266	106	1.00
S-3-1	38	85	3.6	10	136	1.51	2.882	104	1.01
S-3-2	37	85	3.6	10	140	1.51	2.652	106	1.00
S-4-1	36	104	3.4	10	152	1.82	2.451	130	1.21
S-4-2	36	103	3.3	9	156	1.80	2.401	128	1.20

P_{cr} = cracking load, P_u = ultimate load, $S_{r\text{-}av}$ = average crack spacing, $S_{r\text{-}max}$ = maximum crack spacing, N = number of cracks

$\varepsilon_{u\text{-}av}$= average ultimate strain, $\varepsilon_{u\text{-}max}$ = maximum strain at ultimate load and $\varepsilon_{u\text{-}av\text{-}D}$ = average strain at ultimate load for

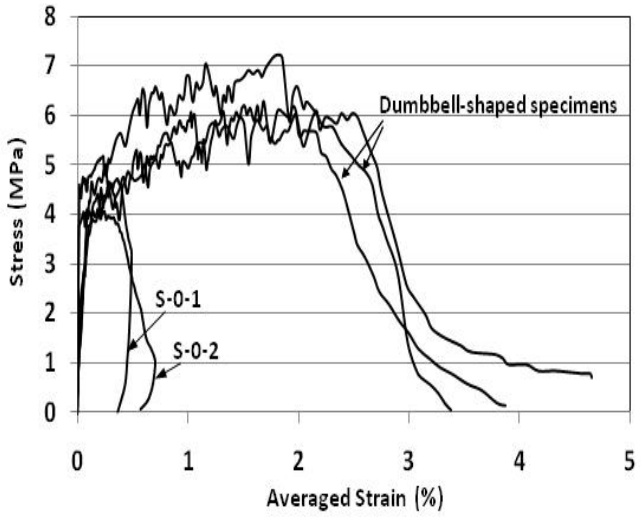

Figure 5. Stress-strain responses for dumbbell-shaped and unreinforced specimens.

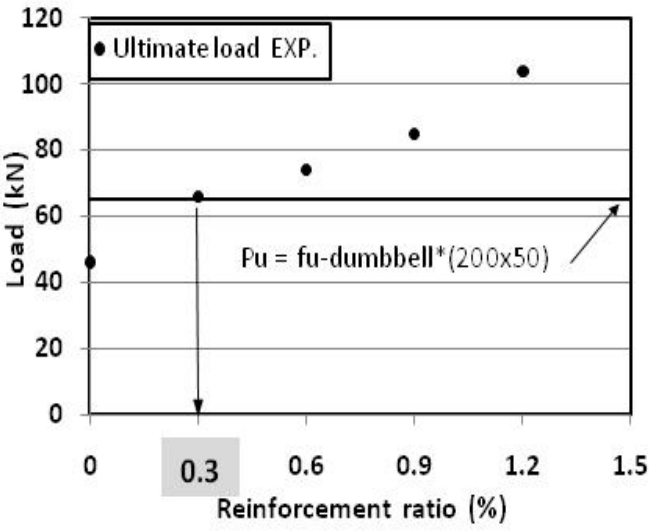

Figure 7. Ultimate load versus reinforcement ratio.

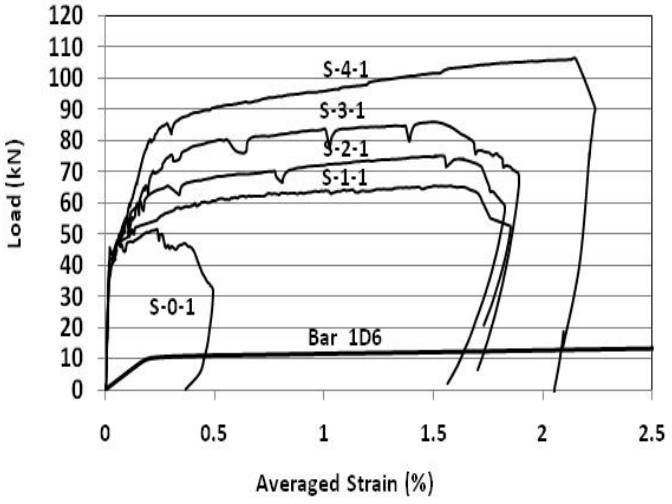

Figure 6. Load-strain responses for tested specimens and a bare bar (1D6).

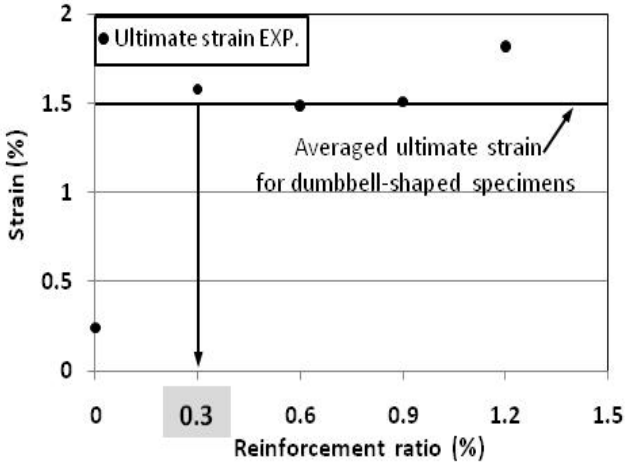

Figure 8. Ultimate strain versus reinforcement ratio.

3 TEST RESULTS AND DISCUSSION

A summary of the experimental results is given in Table 3. As mentioned before, for each reinforcement ratio, two identical specimens were tested. For all cases, the measured experimental data for two identical specimens were found to be very close to one another as shown in Table 3.

3.1 *Effect of specimen's size on stress-strain response*

Figure 5 shows the stress-strain curves for the dumbbell-shaped and unreinforced practical size specimens (S-0-1 and S-0-2). For clarity, only the obtained maximum, minimum and averaged stress-strain responses of the dumbbell-shaped specimens are shown. As can be seen in Figure 5 that the dumbbell-shaped specimens showed the usual elastic and inelastic parts of their stress-strain response (the same stress-strain response was obtained by Kamal 2008). The stress-strain response is linear up to the cracking stress, and thereafter, the stiffness declines significantly and the strain increases rapidly. It is noted that more than 90% of the specimen's ultimate strain (strain at maximum load) was formed after cracking and up to the ultimate load. The specimen's response in this stage (post-cracking stage) is dependent on the reinforcing fibers' properties and orientation. Practical-size specimens (S-0-1 and S-0-2) showed a stress-strain response very similar to that of the dumbbell-shaped specimens up to the cracking stress. However, contrary to the observed response of the dumbbell-shaped specimens, they demonstrated a very limited strain hardening behavior. Comparing the averaged ultimate strain (strain at ultimate load) and stress (ultimate attained load divided by the specimen's cross-sectional area) achieved by the practical size unreinforced specimens and the dumbbell-shaped specimens, an averaged decrease of about 85% and 30% was recorded due to size effect respectively. The stress-strain curves of specimens S-0-1 and S-0-2, shown in Figure 5, demonstrated that the size effect has a fundamental influence on the stress-strain relationship, which can be changed from the conventional response that exhibits strain hardening accompanied by multiple cracking, to sudden failure. This can be attributed to the change in reinforcing fibers' orientation caused by increasing the specimen's thickness. The obtained high tensile properties for the dumbbell-shaped (thickness = 13 mm) specimens may result from the nearly two-dimensional orientation of fibers, which was changed, by increasing the specimen's thickness, to three-dimensional orientation, thereby leading to decreasing of the tensile properties. The effect of increasing the specimen's thickness on orientation of reinforcing fibers was also discussed by Kunieda et al. 2008).

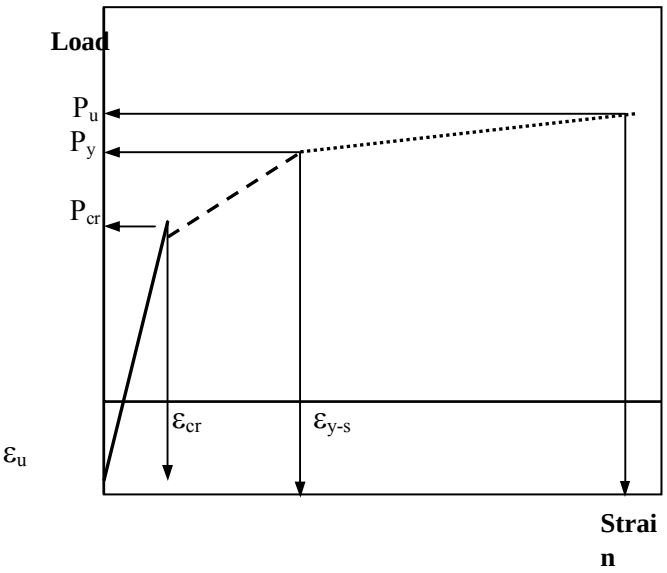

Figure 9. Idealized load-strain response for reinforced UHP-SHCC under axial tension.

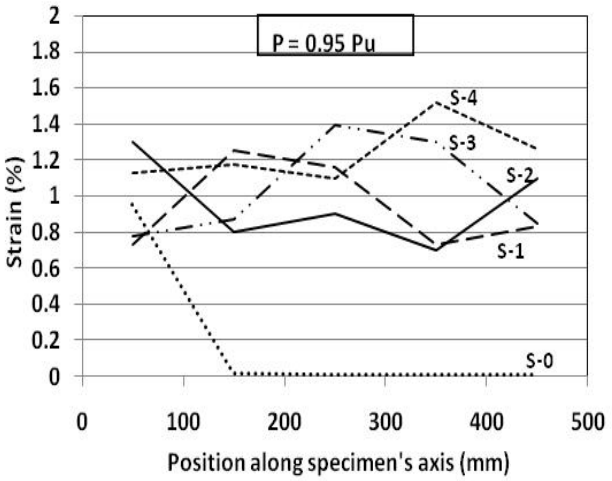

Figure 10. Strain distribution along specimens' axis.

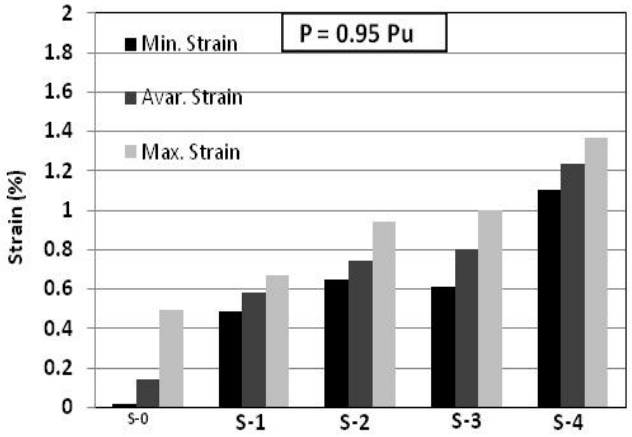

Figure 11. Evaluation results for minimum, maximum and averaged recorded strains.

3.2 *Effect of reinforcement on load-stain relationship*

The averaged strains versus load of the test specimens are illustrated in Figure 6. These strains were obtained by dividing the total elongation of the specimens with their length. For clarity, only the results of one specimen are shown, each two identical specimens show very similar stress versus strain curves. For all the specimens, the load-strain relationship is linear before cracking and the specimens show a very stiff response. After cracking stiffness, however, reduces significantly. It was noted that the response of the unreinforced specimen S-0-1 changed from a conventional ductile failure associated with the formation of multiple fine cracks and large deformations to a more brittle failure associated with a very limited strain hardening response. Contrary to the observed behavior of the unreinforced large size UHP-SHCC specimens, all reinforced UHP-SHCC specimens exhibited strain hardening accompanied by multiple transverse cracking along the specimen's length. The recorded averaged ultimate strain of specimen S-1-1 provided with 0.3% reinforcement ratio was 1.58%, 6.6 times higher than that of unreinforced specimen S-0-1. Moreover, 0.3% reinforcement ratio enabled specimen S-1-1 to outperform the tested dumbbell-shaped specimen's ductility and strength (Fig. 7 and 8). The load-strain response of a bare bar D6 shown in Figure 6 indicates that the increase in reinforced specimens' load carrying capacity is approximately equal to the contribution from steel reinforcement.

For reinforced UHP-SHCC specimens, the response of the load-strain relationship can be divided into three regions as shown in Figure 9. In the first region, the behavior is similar to the unreinforced specimens, since the contribution from the reinforcement is still insignificant. The microcracking increases in the second region, and then a transition zone is entered when the reinforcement is fully activated to counteract the stiffness degradation of UHP-SHCC. The response in this region is mainly dependent on the reinforcement's stiffness and bond between reinforcement and UHP-SHCC. Finally, a third region is recognized in which the strains in the reinforcement exceeds its yielding strain, and the stiffness is generally stabilized around a constant rate.

Figure 10 shows the strain distribution along tested specimens' axis just before failure ($P = 0.95P_u$). The increase in minimum recorded strains, shown in this figure, reveals the ability of the proposed steel reinforcement to preclude the strain localization occurred just after cracking of the unreinforced specimens. Comparing the scatter between the maximum and minimum strains for the

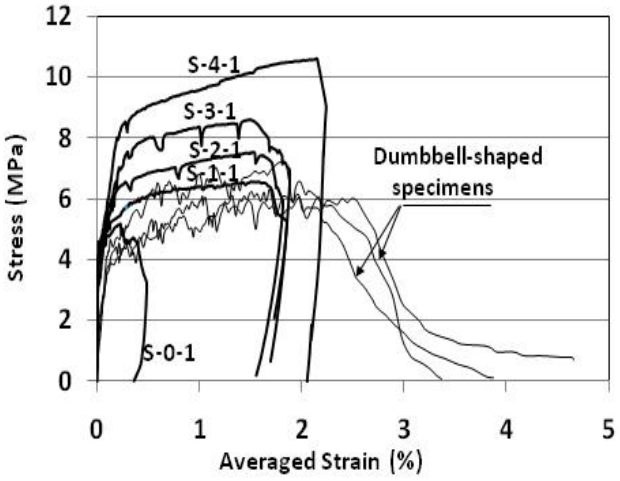

Figure 12. Stress-strain responses for dumbbell- shaped, unreinforced, and reinforced specimens. (including contribution from reinforcement)

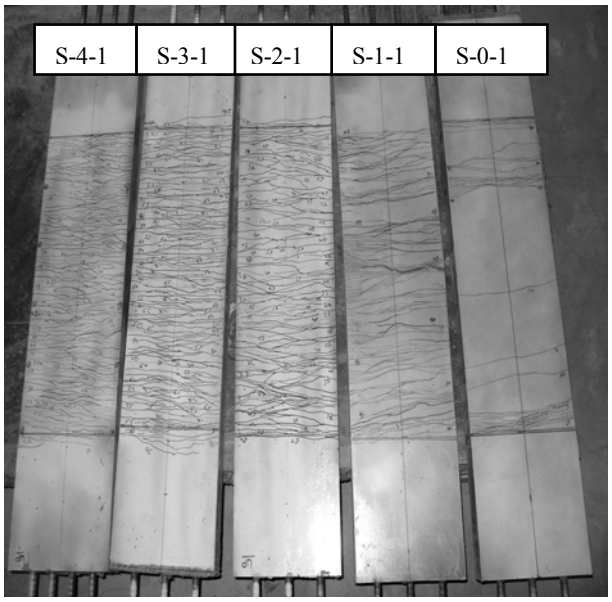

Figure 13. Typical final crack pattern for tested specimens.

reinforced and unreinforced specimens, it was found that a decrease of about 50% was recorded due to 0.3% reinforcement ratio. Also, the minimum recorded strain along the specimen's axis, shown in Figure 11, was increased significantly due to 0.3% reinforcement ratio. Moreover, increasing the reinforcement ratio beyond 0.6% has almost insignificant effect on the minimum attained strains.

Figure 12 shows the nominal stress-strain plots for the tested specimens. The nominal stress was obtained by dividing the applied load by the specimen's cross-sectional area. As can be seen from this figure that the measured ultimate strains and nominal ultimate stresses for specimens S-1 and the dumbbell-shaped specimens were similar to each other. This result suggests that the minimum reinforcement ratio needed to outperform the dumbbell-shaped specimen's ultimate strain and stress, with the given dimensions used in this study is 0.3%.

3.3 *Effect of reinforcement on cracking and ultimate loads*

The cracking and ultimate loads for all the specimens are shown in Table 3. The inverse relation between the cracking load and reinforcement ratio shown in Table 3 can be attributed to the effect of UHP-SHCC shrinkage. Restrained shrinkage caused by internal reinforcement developed tensile stresses which in turn reduced the cracking load. However, the effect of shrinkage on cracking load was insignificant for reinforcement ratio up to 0.6%. Compared to the averaged cracking load of unreinforced specimens, 0.6% reinforcement ratio decreased the cracking load by about 3%.

Comparing the ultimate loads achieved by the tested specimens, it is clear that while increasing the reinforcement ratio the ultimate load will gradually be increased. This is to be expected, because the reinforced specimen's ultimate load is equal to the sum of the contribution from the reinforcing fibers and the steel reinforcement. The greatest increase in ultimate load was obtained in specimen S-4-1, which resulted in a 126% increase over unreinforced specimen S-0-1, followed by specimens S-3-1, S-2-1and S-1-2, exhibiting increases in the ultimate load of 80%, 60% and 40%, respectively. The results seem to indicate that the use of steel reinforcement results in decreasing the reinforcing fibers' stress, just after cracking, and consequently enables the specimen to attain higher ultimate load compared to the unreinforced specimens.

3.4 *Effect of reinforcement on cracking behavior*

The first crack appeared in the specimens once the cracking capacity of the UHP-SHCC was exhausted. With further increases in load, a limited number of transversal cracks formed along the unreinforced specimens' length(S-0-1 and S-0-2). Also, no new cracks formed beyond the load level of 90% of the ultimate load and the crack pattern stabilized at that point. The last crack formed when the load reached 1.05 times its cracking load. Contrary to the observed behavior of specimens S-0-1 and S-0-2, under increasing loads, more transversal cracks formed along the length of all the reinforced UHP-SHCC specimens, and the formation of new cracks continued up to failure of the specimen.

The distinct crack feature of the reference and reinforced specimens, shown in Figure 13, clearly reveals the significant improvement in the crack behavior provided by the proposed steel reinforcement. It can be clearly seen from Figures 14 and 15 and the summary of test results presented in Table 3, that while increasing the reinforcement ratio the average crack spacing will gradually be reduced, whereas the number of developed cracks

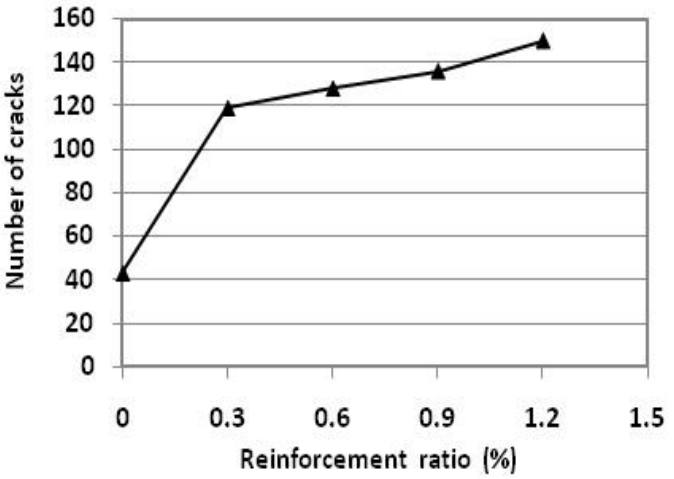

Figure 14. Average crack spacing versus reinforcement ratio for tested specimens.

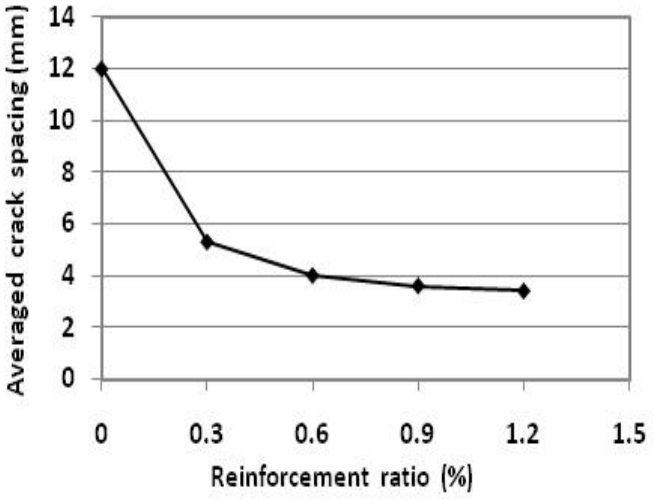

Figure 15. Number of developed cracks versus reinforcement ratio for tested specimens.

was increased. Also, using of 0.3% reinforcement ratio enabled specimen S-1-1 to develop 119 cracks, 2.76 times that of unreinforced specimen S-0-1. It can be also seen that, use of a reinforcement ratio beyond 0.6% has an insignificant effect on the average crack spacing and number of cracks.

The enhancements introduced in the reinforced specimens cracking behavior may be attributed to the increase in axial stiffness at cracks due to the contribution from reinforcement which enables the specimen to carry higher loads and consequently to form more transversal cracks. The results seem to confirm that reinforcing UHP-SHCC tension members with a high modulus of elasticity material such as steel reinforcement helps reduce the reinforcing fibers' stress just after cracking which in turn enables the specimen to carry higher loads (failure of tested specimens was controlled by the occurrence of the fibers debonding). Due to the increase in load carrying capacity all the reinforced specimens were able to develop more cracks compared with unreinforced specimens. Also, specimen S-1-1 demonstrated that the specimen's ultimate load should be at least 1.5

times higher than its cracking load to assure the formation of transversal cracks along its length.

4 CONCLUSIONS

The following conclusions can be drawn from this study:

1-This study demonstrated the effectiveness of the proposed reinforcement to enhance the post-cracking behavior of practical size UHP-SHCC members subjected to axial tension. The averaged strain at ultimate load for specimen S-1 provided with 0.3% reinforcement ratio was 6.6 times that of unreinforced specimen S-0-1.

2-The proposed reinforcement not only increased the ultimate attained strain but also precluded the early localized strain observed for the unreinforced specimens. Comparing the scatter between maximum and minimum strains for the reinforced and unreinforced specimens at ultimate load a decrease of about 50% was recorded due to 0.3% reinforcement ratio.

3-The experimental results show that while increasing the reinforcement ratio the averaged crack spacing will be gradually decreased. However, using of reinforcement ratio beyond 0.6% had an insignificant effect on the averaged spacing and number of cracks.

4-Compared with mode of failure of the dumbbell-shaped specimen, a brittle mode of failure was observed for unreinforced specimens S-0-1 and S-0-2. Once the specimen reached its cracking capacity a limited number of cracks were formed followed by strain localization. Due to this strain localization potential a sudden brittle failure was occurred before the strain hardening of the material was attained.

5- Contrary to the observed behavior of the unreinforced large size UHP-SHCC specimens, all reinforced specimens exhibited strain hardening behavior accompanied by multiple cracking distributed along the specimen's axis. Moreover, 0.3% reinforcement ratio enabled specimen S-1-1 to outperform the dumbbell-shaped specimen's ductility and strength.

6- By increasing the reinforcement ratio, the cracking load was gradually reduced. However; the reduction in cracking load was insignificant for reinforcement ratio up to 0.6%.

REFERENCES

Horii, H., Matsuoka, S., Kabele, P., Takeuchi, S,. Li, V. C. & Kanda, T. 1998. On the prediction Method for the Structural Performance of Repaired/Retrofitted Structures. *Fracture Mechanics of Concrete Structures, FRAMCOS-3 Proceeding*: 1739-1750.

Kamal , A., Kunieda, M., Ueda, N. & Nakamura, H. 2008. Evaluation of Crack Opening Performance of a Repair Material with Strain Hardening Behavior. *Journal of Cement and Concrete Composites.* (30): 863-871.

Kamal, A. 2008. Material Development of UHP-SHCC for Repair Applications and its Evaluation. PhD. Nagoya University.

Kunieda, M. & Rokugo, K. 2006. Recent Progress of HPFRCC in Japan-Required Performance and Applications. *Journal of Advanced Concrete Technology.* 4(1): 19-33.

Kunieda, M., Kamada, T., Rokugo, K. & Bolander, J.,E. 2004. Localized Fracture of Repair material in patch Repair Systems. *Fracture Mechanics of Concrete Structures,FRAMCOS-5 Proceeding:* 765-772.

Kunieda, M., Denarie, E., Bruhwiler, E. & Nakamura, H. 2007. Challenges for Stain Hardening Cementitious Composites-Deformability Versus Matrix Density. *Proceedings of the fifth International RILEM Workshop on HPFRCC* :31-38.

Kunieda, M., Kozawa, K., Ueda, N., & Nakamura, H. 2008. Three-dimensional Meso-scale Analysis for Strain Hardening Cementitious Composites (SHCC). *Creep, Shrinkage and Durability Mechanics of Concrete and Concrete Structures, Proc. of CONCREEP8:* 745-751

Li, V.C. 1993. From Micromechanics to Structural Engineering- The Design of Cementitious Composites for Civil Engineering Applications. *Structural Engineering / Earthquake Engineering,* JSCE. 10(2): 37-48.

Li, V.C. 1998. ECC for Repair and Retrofit in Concrete Structures. *Fracture Mechanics of Concrete Structures, FRAMCOS-3 Proceedin*g:1715-1726

Li, V.C, Horii, H., Kabele, P., Kanda,T. & Lim, Y.M. 2000. Repair and Retrofit with Engineered Cementitious Composites. *International Journal of Engineering Fracture Mechanics.* 65 (2): 317-334.

Li, V. C. 2004. High Performance Fiber Reinforced Cementitious Composites as Durable Material for Concrete Structure Repair. *International Journal for Restoration of Buildings and Monuments.* 10(2): 163-180.

Matsumoto, T. & Mihashi, H. 2002. JCI-DFRCC Summary Report on DFRCC Terminologies and Application Concepts. *Proceedings of the JCI International Workshop on Ductile Fiber Reinforced Cementitious Composites*: 59-66

Maalej M., & Li, V. C. 1995. Introduction of Strain Hardening Engineered Cementitious Composites in the Design of Reinforced Concrete Flexural Members for Improved Durability. *ACI Structural J.* 92(2) :167-176.

Shin S. K., Kim J. J. H. & Lim, Y. M. 2007. Investigation of the strengthening effect of DFRCC applied to plain concrete beams. *Journal of Cement and Concrete Composites.* 29(6): 465-473.